

Transfer Ranking in Finance: Applications to Cross-Sectional Momentum with Data Scarcity

Daniel Poh

Department of Engineering Science,
Oxford-Man Institute of Quantitative
Finance, University of Oxford
Oxford, United Kingdom
dp@robots.ox.ac.uk

Stephen Roberts

Department of Engineering Science,
Oxford-Man Institute of Quantitative
Finance, University of Oxford
Oxford, United Kingdom
sjrob@robots.ox.ac.uk

Stefan Zohren

Department of Engineering Science,
Oxford-Man Institute of Quantitative
Finance, University of Oxford
Oxford, United Kingdom
stefan.zohren@eng.ox.ac.uk

ABSTRACT

Cross-sectional strategies are a classical and popular trading style, with recent high performing variants incorporating sophisticated neural architectures. While these strategies have been applied successfully to data-rich settings involving mature assets with long histories, deploying them on instruments with limited samples generally produce over-fitted models with degraded performance. In this paper, we introduce Fused Encoder Networks – a novel and hybrid parameter-sharing transfer ranking model. The model fuses information extracted using an encoder-attention module operated on a source dataset with a similar but separate module focused on a smaller target dataset of interest. This mitigates the issue of models with poor generalisability that are a consequence of training on scarce target data. Additionally, the self-attention mechanism enables interactions among instruments to be accounted for, not just at the loss level during model training, but also at inference time. Focusing on momentum applied to the top ten cryptocurrencies by market capitalisation as a demonstrative use-case, the Fused Encoder Networks outperforms the reference benchmarks on most performance measures, delivering a three-fold boost in the Sharpe ratio over classical momentum as well as an improvement of approximately 50% against the best benchmark model without transaction costs. It continues outperforming baselines even after accounting for the high transaction costs associated with trading cryptocurrencies.

KEYWORDS

Deep Learning, Transfer Learning, Information Retrieval, Learning to Rank, Neural Networks, Data Scarcity, Factor Investing, Cross-sectional Strategies, Portfolio Construction, Cryptocurrencies

1 INTRODUCTION

Cross-sectional strategies are a popular class of trading strategies that involve first sorting assets by some ranking criteria and then trading the winners against losers. Since the seminal work of [33], which documents the strategy and its performance trading US equities, numerous technical refinements have been introduced. For instance, the ranking step which is at the core of the model evolved from being performed with heuristics [33] to involving more sophisticated DL (Deep Learning) prediction models [28, 35] and modern ranking algorithms such as LambdaMART [9, 50, 63].

Fundamental to calibrating these models is the availability of sufficient data. Whilst this is somewhat mitigated for DL-based strategies operating in the high-frequency domain or for mature

assets with longer trading histories, deploying these strategies on newer instruments is challenging due to their small sample sizes and their degraded performance will likely result in substantial trading losses. Cryptocurrencies, which have recently seen wide interest in both academic and industry, are an example of such a class of instruments.

This dilemma reflects the broader challenge of training DL models that generalise well when confronted with limited data. Although numerous approaches (reducing model complexity [7], few-shot learning [65] and data augmentation techniques [24, 56]) exist for tackling this issue, Transfer Learning stands out as a promising methodology. Transfer Learning focuses on transferring the knowledge obtained across different, but related, source or upstream domains in order to boost the performance of a decision-making function on some target or downstream domains* of interest [21, 70]. It is a broad and active research area, and given the nuances that different problems entail, it overlaps a number of fields such as domain adaptation and multi-task learning†. The multitude of transfer learning successes in computer vision [36, 55] and NLP (natural language processing) [22] tasks have boosted its popularity both as a go-to solution for knowledge transfer problems, as well as a research topic in its own right.

In the space of IR (information retrieval), transfer learning and its closely associated fields has been documented to significantly improve the accuracy of sorting algorithms in target domains with limited samples [14, 15, 26, 41]. However, unlike the computer vision and NLP communities which have rapidly adopted transformer-based solutions in response to their domain-specific transfer learning problems, we note that a corresponding development in IR is surprisingly absent. Inspired by recent works [48, 49] which exploits the Transformer’s attention module to improve ranking performance as well as a first adaptation in the context of finance [51], we similarly make use of this mechanism and propose the Fused Encoder Networks (FEN). Central to the model’s architecture is the usage of dual encoder blocks – one of which is optimised on a larger, but related, upstream dataset and then deployed in conjunction with the other encoder block that is calibrated on a smaller downstream dataset of interest. We focus on applying our transfer ranking model to cryptocurrencies, where relatively short trading

*We use ‘source’ and ‘upstream’ interchangeably. Similarly for ‘target’ and ‘downstream’.

†Domain adaptation is used when the source and target datasets belong in different domains [62]. Multi-task learning is used when the goal is jointly learn a group of related tasks by exploiting the interconnections between tasks [70].

histories (relative to more mature financial instruments) and recent institutional interest promotes them as a pragmatic use-case. Applying cross-sectional momentum across ten cryptocurrencies with the largest market capitalisation, we provide evidence of the superiority of our approach over a set of benchmarks which includes various well-known LTR (Learning to Rank) algorithms. We obtain a threefold boost in Sharpe ratio over classical momentum and a gain of around 50% over the best baseline model. We structure the rest of the paper as follows: The next section discusses related works applying transfer learning to finance as well as ranking tasks. This is followed by Sections 3 and 4 which respectively defines the problem and describes the key elements of the proposed model. We next evaluate the results of our study and finally conclude this work.

2 RELATED WORKS

2.1 Transfer Learning in Finance

Transfer learning focuses on producing an effective model for a target task with scarce training samples by transferring knowledge across different but related source domain(s) [21, 70]. It is an active area of study in machine learning, enjoying success and widespread adoption in various applications [6, 20, 23, 37]. Given the richness of the literature, numerous categorisation schemes have been established to distinguish the various diverse yet inter-connected strands of transfer learning research. For instance, the work in [46] states that depending on the availability of label information, problems in transfer learning can be categorised as transductive, inductive and unsupervised[‡]. Alternatively, depending on whether the source and target domains are represented in similar feature and/or label spaces, transfer learning can be loosely classed as being either homogeneous or heterogeneous [70]. Using the schema in [46], transfer learning techniques can be sorted into 4 groups: instance-based, feature-based, parameter-based and relational-based approaches[§]. Despite these attempts to provide a comprehensive taxonomy of the research landscape, a number of terminology inconsistencies persist – for example, phrases such as domain adaptation and transfer learning are used interchangeably to refer to the same processes [66]. We point our readers to [46, 66, 70] for an better understanding of this broad field.

In the context of transfer learning for finance, most works focus on trading and employ an inductive approach with a parameter-based focus – incorporating the source architecture’s weights and/or model components into the target model in order to optimise learning the task of interest. For instance, [69] propose DeepLOB which is a hybrid deep neural model that predicts stock price movements using high frequency limit order data. In one of the earliest examples of transfer learning in finance, authors document DeepLOB’s

[‡]Inductive transfer learning refers to the scenario where labelled data is available for both the source and target domains. With transductive transfer learning, the labelled source data is available but the labelled target domain data is not. Finally in unsupervised transfer learning, label information is unavailable for both source and target domains.

[§]Instance-based techniques are primarily based on the instance weighting strategy, while feature-based approaches construct a new representation from the original set of features. Parameter-based methods typically involve the transferring knowledge at the model or parameter level. Lastly, relational-based techniques are generally focused on relational problems and extract the rules and/or the logical relationship from the source for use in the target domain.

ability to extract universal features by showing that it is able to successfully transfer learn on a target set of stocks that are not part of the original source training set. The work of [45] develop the RIC-NN (Rank Information Coefficient Neural Net) and demonstrate that the lower layers of the optimised model’s weights in one region (represented by MSCI North America) can be used to initialise the same model for prediction in a different region (MSCI Asia Pacific). In the same vein but with a broader coverage, [38] propose QuantNet which fuses information from different markets with a global bottleneck shared across multiple autoencoder-based architecture; The model then employs a separate decoder for each market to generate market-specific trading strategies. The work in [34] develop a deep Q-learning reinforcement learning trading agent that they combine with pre-trained weights to prevent overfitting that results from insufficient financial data. Concentrating on financial time-series forecasting, [30] tackles the poor performance arising from training deep learning models on limited data by with multi-source transfer learning. In a different setting but utilising a similar pre-trained weights approach, [57] investigates the utility of knowledge transfer methods in evaluating credit risk.

Unlike earlier studies applying transfer learning to the problems in finance, ours differ in a few key aspects. Firstly, while works such as [38, 45] primarily aims to transfer knowledge, ours (along with [30, 34]) is explicitly directed at alleviating the issue of overfitted models that surfaces when calibrating on limited samples. Despite numerous studies focused on applying machine learning techniques to cryptocurrency trading, few, if any, explore the specific use of transfer learning and examine its application over lower frequency settings (such as over weeks) – where the problem of data scarcity is further exacerbated. We address this deficiency in the research with our work in this paper.

2.2 Transfer Ranking

Transfer Ranking (TR) is defined as the application of transfer learning to LTR algorithms [40, 42]. While a plethora of TR algorithms have been developed to address the extensive nature of ranking tasks [13], the primary objectives of these algorithms are essentially similar, i.e. to boost the ranking model’s accuracy on a new collection of items (which we refer to as the target or downstream dataset) by leveraging labelled data from another collection (source or upstream dataset) [40]. From the literature classification in [40], TR techniques can be categorised as either being supervised or unsupervised, with each further divided into homogeneous or heterogeneous depending on the similarity between the source and target feature spaces. Given that our work resembles model adaptation within the space of homogeneous supervised TR techniques, we review works related to this form and point the reader to [40] for details on other setups.

Model adaptation TR concentrates on adapting the existing source model with a few labelled training data from the target collection. Most algorithms concentrating on this form treat the source ranker as a base model, or exploit it as a feature for training [40]. These methods respectively resembles the parameter- and feature-based transfer learning methods in the scheme proposed by [46]. The work in [25], for instance, explores 2 classes of model

adaptation techniques for web search ranking: (i) model interpolation and (ii) error-driven learning approaches based on boosting. The first method learns an ensemble involving both source and target models; In the second, the authors propose LambdaBoost and LambdaSMART [10] which at each boosting iteration adapt the source model to target data (by searching in the spaces of finite basis functions for the former and regression trees for the latter). Other directions undertaken by researchers involve calibrating the source model to better align with the target data. For example, [16] proposes Trada, which is a tree-based model that tunes both weights and splits based on a combination of source and target data. Trada is further improved by incorporating pairwise information to refine the model’s adaptation process [2]. Lastly, [61] adopts a different approach by coefficient transformation. Concretely, the authors develop an algorithm that allows personalised results to be generated by learning a transformation matrix that manipulates the weights of a global ranker.

Surveying the literature surrounding model adaptation TR, solutions employing trees are common. This is likely owing to their flexibility and robustness which has been validated by LambdaMART [9] which is a performance tree-boosting ranking algorithm. While recent LTR breakthroughs, such as [49, 52] provide clear evidence that transformer-based rankers can outperform their tree-based counterparts, we note a lack of models employing this architecture in TR. To this end, we propose the Fused Encoder Networks (FEN) – a novel and hybrid parameter-sharing transfer ranking model that is inspired by the Transformer. The FEN fuses and leverages information that has been flexibly extracted by a pair of encoder-attention modules operating on both source and target domain data. With this design, the model inherits the advantages of self-attention, and can account for dependencies across instruments not just at the loss level during training but also at inference time. By incorporating the components of the source model in the FEN model, the networks hence determines the optimal combination of both source and target information for the ranking task.

3 PROBLEM DEFINITION

This section formalises the problem setting. To get a better idea of the LTR framework as applied to cross-sectional momentum and how TR builds on top of LTR, please refer to Section A in the Appendix.

3.1 Linking Returns and Model Formulation

Given a portfolio of cryptocurrencies that is rebalanced weekly, the returns for a cross-sectional momentum (CSM) strategy at week t can be expressed as follows:

$$r_{t,t+1}^{CSM} = \frac{1}{n} \sum_{i=1}^n S_t^{(i)} \left(\frac{\sigma_{tgt}}{\sigma_t^{(i)}} \right) r_{t,t+1}^{(i)} \quad (1)$$

where $r_{t,t+1}^{CSM}$ refers to the portfolio’s realised returns over weeks t to $t+1$, n denotes the number of cryptocurrencies and $S_t^{(i)} \in \{-1, 0, 1\}$ characterises the CSM signal or trading rule for instrument i . We fix the annualised volatility target σ_{tgt} at 15% and scale returns with $\sigma_t^{(i)}$ which is an estimator for ex-ante weekly volatility. The latter is

computed as the rolling exponentially weighted standard deviation with a 26-week (approximately half a year) span on weekly returns.

The CSM signal S_i in Equation 1 can be obtained using heuristics [33] or by minimising the empirical loss of some prediction model f parameterised by θ :

$$\mathcal{L}(\theta) = \frac{1}{|\Psi|} \sum_{(\mathbf{x}, \mathbf{y}) \in \Psi} \ell(\mathbf{y}, f(\mathbf{x}; \theta)) \quad (2)$$

With slight abuse of notation, we take each item x_i to be a k -sized real-valued feature vector. Since \mathbf{x} is a list of n items, we have $\mathbf{x} \in \mathbb{R}^{n \times k}$. The training data is denoted as $\Psi = \{(\mathbf{x}, \mathbf{y}) \in \mathbb{R}^{n \times k} \times \mathbb{Z}_+^n\}$, where \mathbf{y} is a list of n bins for the same \mathbf{x} sorted by realised returns for the *next* period. When the prediction model f adopts a regress-then-rank approach such as [28, 35], then the loss function ℓ is usually the pointwise MSE (mean squared error). With LTR models, pairwise and listwise losses that accounts for the mutual interaction among objects are usually used for ℓ .

3.2 Model Formulation under the Transfer Ranking Framework

With parameter-based transfer learning approaches, an upstream or source model is first trained on the source data. This can be expressed as:

$$\mathcal{L}(\theta_S) = \frac{1}{|\Psi_S|} \sum_{(\mathbf{x}, \mathbf{y}) \in \Psi_S} \ell(\mathbf{y}, f_S(\mathbf{x}; \theta_S)) \quad (3)$$

where the terms f_S , θ_S and Ψ_S are respectively the prediction model, its parameter vector and the associated dataset. The tuned upstream weights are next incorporated into the downstream or target model:

$$\mathcal{L}(\theta_T) = \frac{1}{|\Psi_T|} \sum_{(\mathbf{x}, \mathbf{y}) \in \Psi_T} \ell(\mathbf{y}, f_T(\mathbf{x}; \theta_S, \theta_T)) \quad (4)$$

where adhering to the form laid out by Equation 2, f_T refers to the ranking function parameterised by both source and target parameters θ_S as well as θ_T , and ℓ is either a pairwise or listwise loss. In the final fine-tuning step, minimising the loss can be formulated as:

$$\mathcal{L}(\tilde{\theta}_S, \theta_T) = \frac{1}{|\Psi_T|} \sum_{(\mathbf{x}, \mathbf{y}) \in \Psi_T} \ell(\mathbf{y}, f_T(\mathbf{x}; \tilde{\theta}_S, \theta_T)) \quad (5)$$

and $\tilde{\theta}_S$ denotes the subset of parameters within θ_S that is permitted to be fine-tuned. Using this final model, we compute ranking scores which we then sort and threshold to obtain the cross-sectional trading signal S_t required for portfolio construction. Figure 1 visualises the TR pipeline and compares it to traditional LTR.

4 FUSED ENCODER NETWORKS

Optimising the FEN (Fused Encoder Networks) involves first training a source model on a larger dataset. The calibrated components are then shared with the target model (i.e., FEN) as part of a broader framework. The following section provides key details and explain how various components come together.

4.1 Source Model Architecture

We use a stacked encoder block with a linear projection applied to inputs (similar to [49, 50]) as our source model. Each encoder within the stack is a composite layer housing the attention mechanism

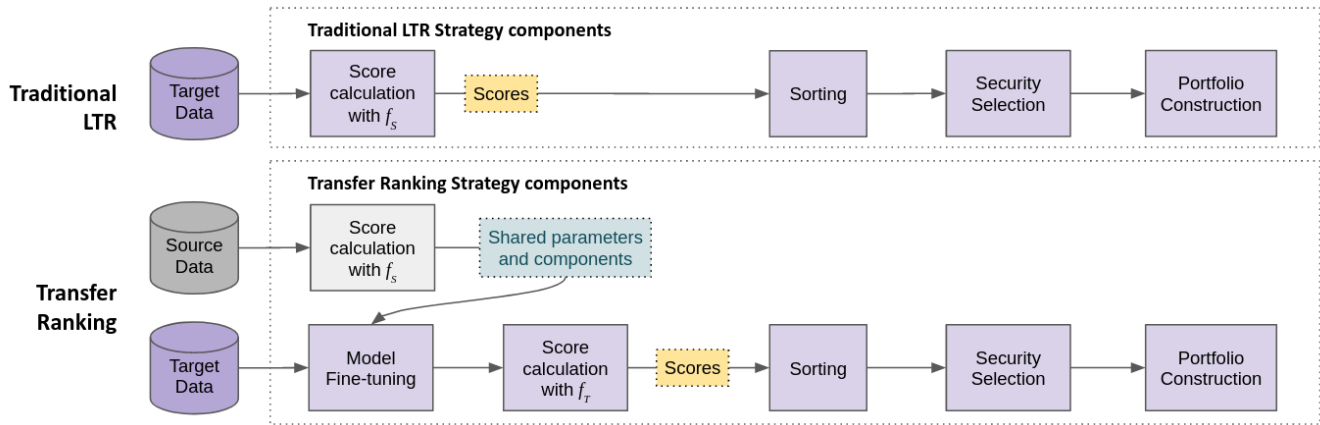


Figure 1: Pipelines for traditional LTR (top) and Transfer Ranking (bottom): The latter involves first training a source (upstream) model on a different but related dataset, and then transferring the knowledge by sharing the calibrated weights/components with a target (downstream) model. Apart from requiring an additional fine-tuning step, the training process for the target model follows that of traditional LTR.

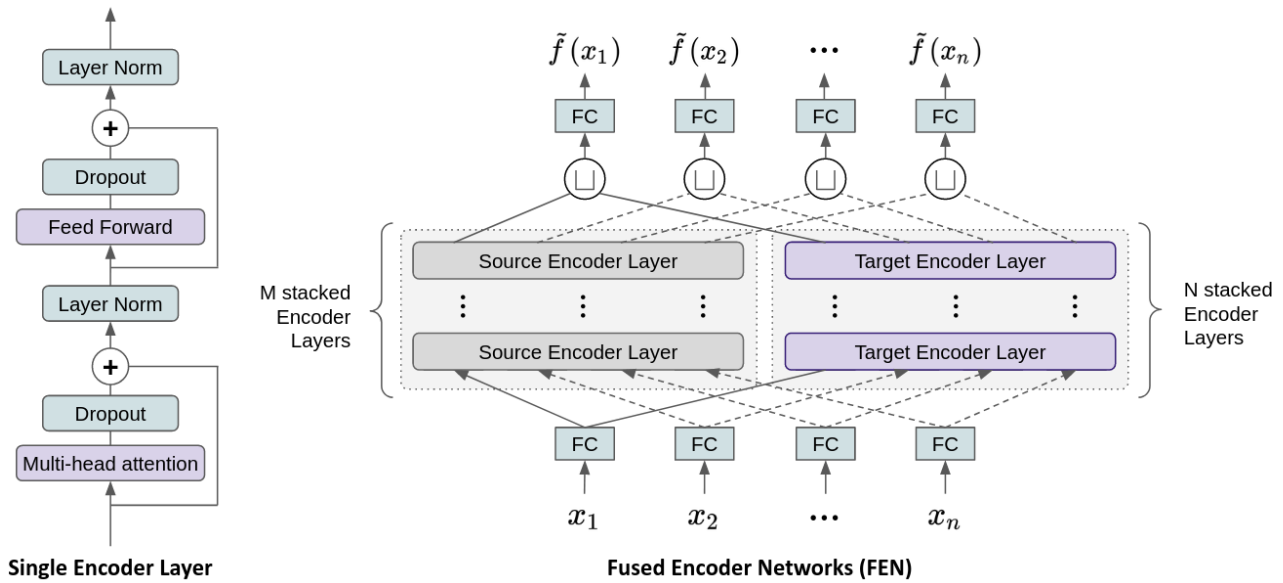


Figure 2: Architecture of a single Encoder Layer (left) as well as the FEN (Fused Encoder Networks) (right). Each single Encoder Layer is composed of a multi-head attention module and a feed forward network and uses dropouts and layer normalisation to learn higher order feature representations. The FEN is composed of both the source and target encoder blocks running in parallel. The \sqcup symbol represents the concatenate operator.

and a feed-forward network that enables it to learn higher-order feature representations. It is a key component in both the source and target models (See left of Figure 2)

4.1.1 Feed-forward Network. This component introduces non-linearity via its ELU (Exponential Linear Unit) [18] activation. It also facilitates interactions across different parts of its inputs.

4.1.2 Self-Attention and Multi-head Attention. The attention mechanism is a function that maps a query and a key-value pair to an

output. While a few variants of attention exist, we use the form similar to that employed in the Transformer, which is the scaled dot-product attention followed by a softmax operation [60]:

$$\text{Att}(\mathbf{Q}, \mathbf{K}, \mathbf{V}) = \text{softmax}\left(\frac{\mathbf{Q}\mathbf{K}^T}{\sqrt{d_{\text{model}}}}\right)\mathbf{V} \quad (6)$$

where \mathbf{Q} , \mathbf{K} and \mathbf{V} are respectively the query, key and value matrices. In *self*-attention, the *same* inputs are used for all three matrices. Combining multiple attention units produces the multi-head

attention module which boosts the model’s capacity to learn representations:

$$\text{MHA}(\mathbf{Q}, \mathbf{K}, \mathbf{V}) = \text{concat}(\text{head}_1, \dots, \text{head}_h) \mathbf{W}^O \quad (7)$$

$$\text{head}_i = \text{Att}(\mathbf{Q} \mathbf{W}_i^Q, \mathbf{K} \mathbf{W}_i^K, \mathbf{V} \mathbf{W}_i^V) \quad (8)$$

where in the above equations, each head_i (out of h heads) refers to the i th attention mechanism of Equation 6, and learned parameter matrices:

$$\begin{aligned} \mathbf{W}_i^Q &\in \mathbb{R}^{d_{\text{model}} \times d_q}, & \mathbf{W}_i^K &\in \mathbb{R}^{d_{\text{model}} \times d_k}, \\ \mathbf{W}_i^V &\in \mathbb{R}^{d_{\text{model}} \times d_v}, & \mathbf{W}^O &\in \mathbb{R}^{hd_v \times d_{\text{model}}} \end{aligned}$$

where typically $d_q = d_k = d_v = d_{\text{model}}/h$ is used.

4.1.3 Stacking Encoder Layers. A single encoder block $\xi(\cdot)$ can be expressed as:

$$\xi(\mathbf{x}) = \Gamma(\mathbf{z} + \delta(\phi(\mathbf{z}))) \quad (9)$$

$$\mathbf{z} = \Gamma(\mathbf{x} + \delta(\text{MHA}(\mathbf{x}))) \quad (10)$$

where $\Gamma(\cdot)$, $\delta(\cdot)$ and $\phi(\cdot)$ refers to the layer normalisation operation, a dropout function and a projection onto a fully-connected layer respectively. Additionally, $\text{MHA}(\cdot)$ represents the multi-head attention module. Stacking multiple encoder layers enables the model to learn more complex representations:

$$\xi(\mathbf{x}) = \xi_1(\dots(\xi_N(\mathbf{x}))) \quad (11)$$

where $\xi(\mathbf{x})$ in Equation 11 characterises a stacked encoder involving a series of N encoder layers.

4.2 Target Model Architecture

With conventional parameter sharing techniques, if a neural model is used to learn the source task, then a target model can be constructed by directly retaining most of its layers [70]. Motivated by the empirical superiority of context-aware LTR models using the attention mechanism over standard rankers [49, 51], we utilise a hybrid approach – running the pre-trained source Transformer’s encoder block $\xi_S(\cdot)$ as an additional feature extractor operating in *parallel* with the target Transformer’s block $\xi_T(\cdot)$:

$$\xi_S(\mathbf{x}) = \xi_{S_1}(\dots(\xi_{S_M}(\mathbf{x}))) \quad (12)$$

$$\xi_T(\mathbf{x}) = \xi_{T_1}(\dots(\xi_{T_N}(\mathbf{x}))) \quad (13)$$

where ξ_{S_i} and ξ_{T_j} are respectively the i th and j th encoder layer from the source and target model (See the right of Figure 2). Against standard parameter-sharing methods, our setup has the additional advantage of being plug-and-play, allowing to be appended anywhere to any pre-trained network. The outputs from both encoder blocks are concatenated:

$$\xi_{S,T}(\mathbf{x}) = \text{concat}(\xi_S(\mathbf{x}), \xi_T(\mathbf{x})) \quad (14)$$

before projecting onto a fully connected layer to obtain our raw score predictions $f(\mathbf{x})$. Although we use a simple projection for simplicity, this can be replaced by more complex processing such as those that involve deep or cross networks [64].

4.3 Loss Function

We optimise both the source and target transformers with the ListNet loss [11] and note that other losses such as ListMLE [68] or metrics like ApproxNDCG [8] can be used. The ListNet loss is defined as:

$$\ell(\mathbf{y}, f(\mathbf{x})) = - \sum_i \text{softmax}(\mathbf{y})_i \times \log(\text{softmax}(f(\mathbf{x}))_i) \quad (15)$$

4.4 Model Fine-tuning

Deep networks can be fine-tuned in several ways. One simple approach is to optimise all the parameters of the model after initialising it with the pre-trained model’s parameters. Another method, which is driven by the findings that learned features transition from general to specific along a network [43], concentrates on re-training only the last few layers while leaving the parameters of the remaining initial layers frozen (at their pre-trained values). There are also other methods, such as [27] and [53]. As the number of layers to freeze is a manual design choice which introduces an unnecessary complexity, we do not freeze any layers and instead focus on re-training the entire model with a low learning rate.

5 PERFORMANCE EVALUATION

5.1 Dataset Overview

For actual performance evaluation, all models utilise daily closing prices obtained from CoinMarketCap [19] that is further downsampled[¶] to the weekly frequency. We define our universe to be the top 10 cryptocurrencies in terms of market capitalisation as of the end of Dec-2019, with at least 4 years of price history. Given the limited size of the data, this selection ensures sufficient samples for model training and to draw meaningful inference. We fix this set of cryptocurrencies from the end of Dec-2019 up until the end of Dec-2021 set to minimise the impact of survivorship bias. The full data set thus runs from 1-Jan-2016 to 31-Dec-2021, with 2018 and 2021 being the first and last target test years respectively.

To train the source model needed for knowledge transfer, we make use of the same set of daily data relating to 30 currency pairs^{¶¶} as per [4, 51] obtained from the Bank for International Settlements (BIS) [3] spanning May-2000 to Dec-2021 which we again downsample to the weekly frequency. To measure risk aversion, we use the daily close of the VIX historical data from the Cboe Global Markets [12], where a week is labelled risk-off if it contains one or more days when the VIX is 5% higher than its 60-day moving average. A normal week is thus a non-risk-off week. For further details about the data, we refer the reader to Section B in the Appendix.

5.2 Predictor Description

Our portfolios are rebalanced weekly, and we construct an equally weighted long/short portfolio with the top/bottom 2 cryptocurrencies. For predictors across both source and target models, we use a simple set of returns-based features. The source model is trained with the following features:

[¶]We downsample to Wednesday every week to avoid excessive loss of data.

^{¶¶}Indeed, it can be argued that other source data sets are more suitable for pre-training given the objective of this study. Returns on technology stocks might be one such example. We leave this for future research.

- (1) *Raw returns* – Raw FX returns over the past 1, 2, 3 and 4 weeks, making use of the findings of [44].
- (2) *Normalised returns* – Raw FX returns over the previous 1, 2, 3 and 4 weeks standardised by weekly volatility scaled to the appropriate time scale.

For the target model, we again use both raw and normalised cryptocurrency returns but only over the past 1, 2 and 3 weeks as evidence of significant momentum returns in cryptocurrencies is mixed using a 1-month formation period [58].

5.3 Models and Comparison Metrics

- (1) 1-week Returns (1WR) – This is based on the findings of [58] and is analogous to the classical equity momentum strategy of [33]. Unlike the original approach of [58] however, we do not form overlapping portfolios but instead construct weekly long/short portfolios based on returns over the previous 1 week. The final portfolio is then scaled to the desired target volatility.
- (2) Multi-Layer Perceptron (MLP) – Characterises the typical Regress-then-rank model used by contemporary strategies.
- (3) ListNet (LN) – Listwise Learning to Rank model proposed by [11].
- (4) LambdaMART (LM) – Pairwise Learning to Rank model proposed by [9].
- (5) Self-attention based Ranker (SAR) – This benchmark uses the Transformer’s encoder module for ranking and is directly applied to the cryptocurrency data. The use of the Transformer’s encoder for ranking was initially proposed by [49] in an IR setting, and was later applied to constructing cross-sectional strategies by [51]**.
- (6) SAR with Parameter-Sharing (SAR+ps) – This involves pre-training the Transformer’s encoder module on the larger FX dataset and then fine-tuning on the target cryptocurrency set. Fine-tuning pre-trained models has been documented to be a valid and successful transfer learning approach for computer vision [70] and NLP [22, 31] tasks.
- (7) Fused Encoder Networks (FEN) – The proposed model.

We assess the the models over four key areas (profitability, risk-iness, risk-adjusted performance and ranking accuracy) with the following metrics:

- Profitability: Expected returns ($\mathbb{E}[\text{Returns}]$) and Hit rate (percentage of positive returns at the portfolio-level obtained over the out-of-sample period).
- Risks: Volatility, Maximum Drawdown (MDD) and Downside Deviation.
- Financial Performance: Sharpe $\left(\frac{\mathbb{E}[\text{Returns}]}{\text{Volatility}}\right)$, Sortino $\left(\frac{\mathbb{E}[\text{Returns}]}{\text{MDD}}\right)$ and Calmar $\left(\frac{\mathbb{E}[\text{Returns}]}{\text{Downside Deviation}}\right)$ ratios are used as a gauge to measure risk-adjusted performance. We also include the average profit divided by the average loss $\left(\frac{\text{Avg. Profits}}{\text{Avg. Loss}}\right)$.
- Ranking Performance: NDCG@2. This is based on the Normalised Discounted Cumulative Gain (NDCG) [32] which is a measure of graded relevance. We focus on assessing

the NDCG of the top/bottom 2 cryptocurrencies which are directly linked to strategy performance.

5.4 Training and Backtest Details

5.4.1 Benchmark Models. With the exception of 1WR and LM, all models are tuned with minibatch stochastic gradient descent with the Adam optimiser. All machine-learning based models are calibrated using an expanding window approach in one year blocks^{††}. Backpropagation was conducted for a maximum of 100 epochs and with an expanding window approach, where 90% of a given training block is used for training and remainder for validation. Early stopping was used to prevent overfitting and is triggered when the validation loss does not improve for 25 epochs. Model hyperparameters were tuned over 50 iterations of search using HyperOpt [5]. Further details relating to model calibration can be found in Section C of the Appendix.

5.4.2 Fused Encoder Networks. The FEN is optimised in 3 steps. The upstream model is first calibrated on the source FX data. This is performed with a one-year expanding window approach where we test our strategy on a given year, and use all preceding samples for model tuning with a 90%/10% train/validation split. For the next year, we expand and shift the training and test periods respectively.

For the next step, the source model’s encoder block is transferred to the FEN and trained on the target data with the source block frozen. Similar to source model training, the FEN is trained using a single-year expanding window with a 90%/10% split. To minimise any detrimental effects arising from *negative transfer*, which is the case when the transferred source knowledge adversely impacts performance on the downstream task, we first proceed as follows: to generate predictions for each out-of-sample year t on the target task, we produce 10 runs of the source models evaluated on $t - 1$. We pick the source model with the *highest* Sharpe ratio, and use it to train the target model (as we evaluate model performance (discussed later) based on 10 runs, we pick the top 2 source models and go on to train 5 target models with each.). This process is illustrated in Figure 3. The consequences of transferring knowledge from models with the *lowest* Sharpe ratios can be found in Section D of the Appendix.

The final fine-tuning phase optimises the unfrozen network with a very low learning rate – set as the smallest value in the search space for learning rates. The model is run for a maximum of 100 epochs and is stopped early if the validation loss fails to improve for 10 epochs. We fine-tune only the FEN and SAR+ps. Further details can be found in Section C of the Appendix.

5.5 Results and Discussion

5.5.1 Trading Performance. Table 1 consolidates trading performance across the various strategies after 10 runs^{‡‡}. While the

^{††}Using the first iteration as an example – we retain 90% of the 2016-2017 period for training and use remainder for cross-validation, with 2018 held out for testing. In the next iteration, the training set is expanded to include 2018 (i.e., 2016 to 2018) and the model is tested using 2019. See also Figure 3.

^{‡‡}The results of 1WR are obtained after a single run as there is no stochastic training involved. All other models are based on 10 runs. For rankers that use transfer learning, i.e. SAR+ps and FEN, we produce a set of 10 source models for each. With each set, we pick the top 2 ranked by the Sharpe ratio and go on to train 5 target models with each.

**We use the variant without positional encodings as we are not performing re-ranking.

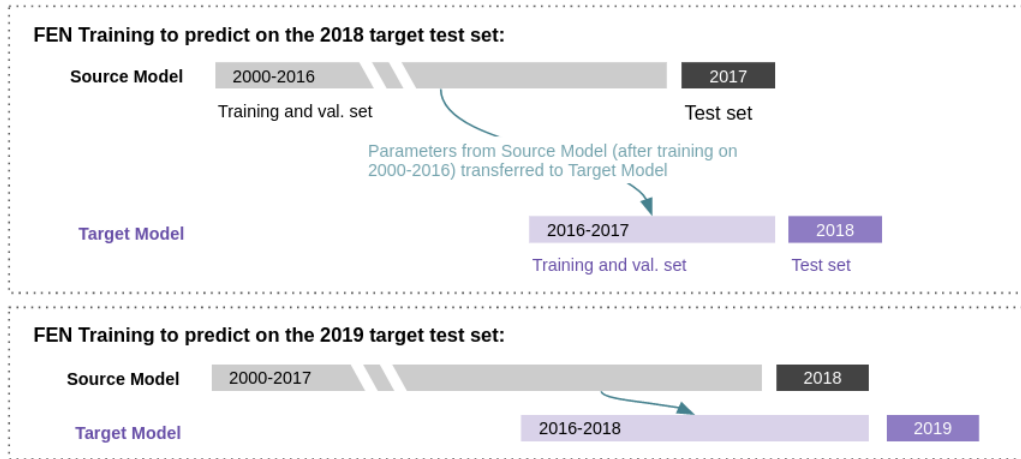


Figure 3: Source and target (FEN) model training. Both the source and target models are trained using an expanding window of one-year blocks. To minimise any impact of negative transfer, we assess the performance of the upstream model on the year preceding the target test year and only use models that have performed well for knowledge transfer.

Table 1: Performance metrics for all models over the out-of-sample 2018–2021 period, rescaled to match a 15% annual volatility target. All figures except for those belonging to 1WR are computed based on 10 runs. FEN outperforms the benchmark models on nearly all measures.

	Benchmarks						Proposed
	1WR	MLP	LN	LM	SAR	SAR+ps	FEN
E[returns]	0.053	0.080±0.043	-0.094±0.132	0.076±0.109	0.084±0.100	-0.006±0.074	*0.141±0.080
Volatility	0.221	0.201±0.033	0.211±0.087	0.205±0.068	*0.176±0.015	0.178±0.012	0.187±0.012
Sharpe Ratio	0.238	0.403±0.240	-0.397±0.539	0.456±0.546	0.496±0.583	-0.035±0.406	*0.749±0.410
Sortino Ratio	0.484	0.692±0.436	-0.405±0.745	0.943±1.061	0.937±1.070	0.028±0.597	*1.526±1.023
Calmar Ratio	0.190	0.373±0.231	-0.109±0.364	0.439±0.546	0.454±0.543	0.027±0.205	*0.828±0.543
Downside Deviation	0.109	0.125±0.039	0.173±0.098	0.132±0.081	0.115±0.029	0.122±0.022	*0.102±0.017
Max. Drawdown	0.276	0.248±0.084	0.443±0.153	0.285±0.115	0.272±0.097	0.356±0.113	*0.188±0.036
Avg. Profit / Avg. Loss	*1.417	1.175±0.155	0.840±0.194	1.172±0.239	1.190±0.211	1.068±0.187	1.342±0.275
Hit Rate	0.435	0.499±0.030	0.481±0.035	0.505±0.026	0.500±0.029	0.472±0.019	*0.509±0.031

statistics here are computed without transaction costs to focus on raw performance, we consider the impact of different cost assumptions later in Section 5.5.4. An additional layer of volatility scaling is applied at the portfolio level to facilitate comparison. Where applicable, each bold and asterisked figure indicate the best measurement across all models for its respective performance measures.

The statistics presented in Table 1 demonstrate the superiority of the FEN model – delivering an approximately threefold boosting of the Sharpe ratio relative to the heuristics-based 1WR and an improvement of about 50% versus the best benchmark (SAR). From a risk perspective, FEN is among the least volatile and possesses the lowest downside deviation and max drawdown figures. We also note that the instability associated with cryptocurrencies is reflected across all models running at levels higher than the 15% annual target.

Focusing on the reference baselines, SAR and LN are respectively the best and worst models. While SAR’s performance is likely assisted by its sophisticated underlying model, it is only marginally

better than the tree-based LM. Additionally, the consequence of naively training neural models on extremely limited samples is reflected in LN’s results – which are significantly worse than the simpler 1WR model. While both SAR and SAR+ps share the same transformer-based architecture, the latter’s inferiority suggests that *only* relying on a network pre-trained on FX data is insufficient in the context of this work. In FEN, the pre-trained network runs in *parallel* with the target encoder block. This leads to the model behaving like an ensemble of (potentially shallow) networks and avoids depending *solely* on the pre-trained module – which can be catastrophic for performance when affected by negative transfer (See Appendix Section D) – and instead allows extracted features to be flexibly combined in a data-driven manner.

5.5.2 Ranking Performance. We assess ranking precision with the NDCG (Normalised Discounted Cumulative Gain) which is popular measure in the IR literature, and with higher values implying greater accuracy in sorting objects (to match some optimal ordering). Given

that we trade the top/bottom quintile each time, we concentrate on the average NDCG@2 for both long and short trades aggregated over all weekly rebalances. Table 2 indicates that the MLP is able to rank the most accurately based on this measure, and this followed by FEN. Although better accuracy generally implies higher returns and Sharpe ratios as seen in Table 1, this does not hold for the MLP. This inconsistency can be resolved when we group FEN’s returns conditioned on the relative accuracy (over rebalances) of the FEN against the MLP^{§§}. By segmenting returns and accuracy in this manner, we observe that FEN is only slightly worse off returns-wise when it is less accurate than the MLP, but generate considerably higher returns when it is more accurate – which explains its higher overall returns (and Sharpe ratio). These results are presented in Table 3.

5.5.3 Attention Heatmap Patterns. Attention is an integral part of various state-of-the-art Transformer-based architectures, providing these models with an effective way to model relationships by attending to relevant regions in the data. To determine if the attention mechanism of our proposed model is able to learn useful information, we examine their raw attention heatmaps. Specifically, we visualise the *last* attention layer of the model’s target encoder stack since deeper layers tend to capture high-level representation and global relationships [47]. Against the backdrop of increasingly coupled markets, volatility spillovers have grown increasingly frequent such as risk transmission from the equity to cryptocurrency markets [59]. Figure 4 depicts the aggregated heatmaps across normal and global risk-off regimes^{¶¶}. Darker cells correspond to larger weights which plays a larger role in the model’s prediction^{***}. The heatmaps show that the darker cells are more dispersed in risk-off states since multiple instruments are affected. This pattern of dispersion is less evident over normal states – likely a result of idiosyncratic developments in the cryptocurrency markets.

Beyond the impactful macro-level episodes that cause sharp changes to the VIX, we observe similar behaviour of the FEN’s attention mechanism at significant cryptocurrency-specific market events as well. In the left of Figure 5 for instance, a distinct darker column of cells over Dogecoin formed around the time of Elon Musk’s tweet about the digital token [67]. On the right heatmap, the dispersed region of darker cells reflects the risk-off sentiments inherent in China’s regulators’ intent to crack down on the use of cryptocurrencies [29]. These plots indicate that FEN’s attention module is responsive to market dynamics and is capable of learning useful information. More importantly, they appear to possess an interpretable structure and provide an additional perspective that helps explain its strong performance against other attention-based benchmarks. We refer the interested reader to Section E of the Appendix to see how the heatmaps of other models compare.

^{§§}The MLP has a higher average NDCG@2 than FEN for about 52% of the times when the portfolio is rebalanced.

^{¶¶}We define a risk-off event at the weekly frequency as an instance when the daily VIX over any one or more days within the week is 5% points higher than its 60-day moving average, and all normal states are thus defined to be non-risk-off states. This definition classifies approximately 20% of the target dataset’s evaluation period as risk-off.

^{***}We also note that attention has been documented by [54] to be a noisy indicator of a model inputs’ overall contribution to final prediction, and is not a fail-safe measure. Additionally, the heatmaps are not symmetric due to the softmax operator used in computing attention.

5.5.4 Turnover Analysis. To investigate the impact of transaction costs on strategy performance, we first compute the weekly portfolio turnover at period t which we define as:

$$\zeta_t^{(i)} = \sigma_{tgt} \sum_{i=1}^n \left| \frac{S_t^{(i)}}{\sigma_t^{(i)}} - \frac{S_{t-1}^{(i)}}{\sigma_{t-1}^{(i)}} \right| \quad (16)$$

Table 4 shows the FEN model as among the strategies with the lowest average turnover over 2018-2021. To further examine and quantify the impact of transaction cost on performance, we also compute the ex-cost Sharpe ratios and present the results in Table 5. The figures show that FEN is able to deliver higher and positive cost-adjusted Sharpe ratios up to 29 bps – above the 26 bps per trade assumed for cryptocurrencies [58] and therefore demonstrating its suitability for trading these instruments.

6 CONCLUSION

We introduce Fused Encoder Networks (FEN) – a novel and hybrid parameter-sharing transfer ranking model that overcomes the issue of over-fitted cross-sectional strategies based on neural rankers to trade instruments with short histories. Using the popular momentum strategy applied to cryptocurrencies as a demonstrative use-case, we validate the effectiveness of our proposed approach. Concretely, the FEN surpasses the reference baselines on most performance measures – notably delivering an approximately threefold boosting of the Sharpe ratio over classical momentum and a gain of approximately 50% over the best benchmark. Future work includes modifying various components of the original framework, such as introducing additional processing in the output head or replacing the listwise loss with other loss functions. Another direction is to explore transferring and synthesising knowledge from other/multiple source domains.

ACKNOWLEDGMENTS

We would like to thank the Oxford-Man Institute of Quantitative Finance for financial and computing support. SR is grateful for support from the Royal Academy of Engineering.

REFERENCES

- [1] Martin Abadi, Ashish Agarwal, Paul Barham, Eugene Brevdo, Zhifeng Chen, Craig Citro, Greg S. Corrado, Andy Davis, Jeffrey Dean, Matthieu Devin, Sanjay Ghemawat, Ian Goodfellow, Andrew Harp, Geoffrey Irving, Michael Isard, Yangqing Jia, Rafal Jozefowicz, Lukasz Kaiser, Manjunath Kudlur, Josh Levenberg, Dandelion Mané, Rajat Monga, Sherry Moore, Derek Murray, Chris Olah, Mike Schuster, Jonathon Shlens, Benoit Steiner, Ilya Sutskever, Kunal Talwar, Paul Tucker, Vincent Vanhoucke, Vijay Vasudevan, Fernanda Viégas, Oriol Vinyals, Pete Warden, Martin Wattenberg, Martin Wicke, Yuan Yu, and Xiaoqiang Zheng. 2015. TensorFlow: Large-Scale Machine Learning on Heterogeneous Systems. <https://www.tensorflow.org/> Software available from tensorflow.org.
- [2] Jing Bai, Fernando Diaz, Yi Chang, Zhaohui Zheng, and Keke Chen. 2010. Cross-market model adaptation with pairwise preference data for web search ranking. In *Proceedings of the 23rd international conference on computational linguistics: Posters (COLING '10)*. Association for Computational Linguistics, USA, 18–26. Number of pages: 9 Place: Beijing, China.
- [3] (BIS) Bank for International Settlements. 2022. US dollar exchange rates. *Calculated (or Derived) based on BIS data.* (2022). <https://www.bis.org/statistics/xrusd.htm>
- [4] Jamil Baz, Nicolas M Granger, Campbell R. Harvey, Nicolas Le Roux, and Sandy Rattray. 2015. Dissecting Investment Strategies in the Cross Section and Time Series. *SSRN Electronic Journal* (2015). <https://doi.org/10.2139/ssrn.2695101>
- [5] James Bergstra, Brent Komer, Chris Eliasmith, Dan Yamins, and David D Cox. 2015. Hyperopt: A Python Library for Model Selection and Hyperparameter

Table 2: Ranking performance for all models based on the popular NDCG (Normalised Discounted Cumulative Gain). We calculate the average NDCG@2 over long and short positions across all rebalances. All figures except for those belonging to 1WR are computed based on 10 runs. Higher accuracy typically translates to higher returns and Sharpe ratios (See Table 1). FEN outperforms most benchmarks in terms of NDCG@2 except for the MLP.

	Benchmarks						Proposed
	1WR	MLP	LN	LM	SAR	SAR+ps	FEN
NDCG@2	0.580±0.198	*0.615±0.007	0.597±0.010	0.601±0.007	0.604±0.010	0.594±0.007	0.607±0.011

Table 3: Segmented returns based on the relative ranking performances of the MLP and FEN models. We calculate the average NDCG@2 over long and short positions across all rebalances. The first 2 columns compare these measures at the times when FEN has an NDCG@2 lower (i.e., less accurate) than the MLP. The next pair of columns compare the same measures over instances when FEN has a higher NDCG@2. The magnitude of FEN’s gains (when more accurate than the MLP) are larger than its losses (when less accurate).

	MLP more accurate		FEN more accurate	
	MLP	FEN	MLP	FEN
NDCG@2	0.648±0.115	0.566±0.117	0.576±0.108	0.648±0.105
Avg. Returns	0.006±0.023	0.000±0.020	-0.004±0.016	0.006±0.014

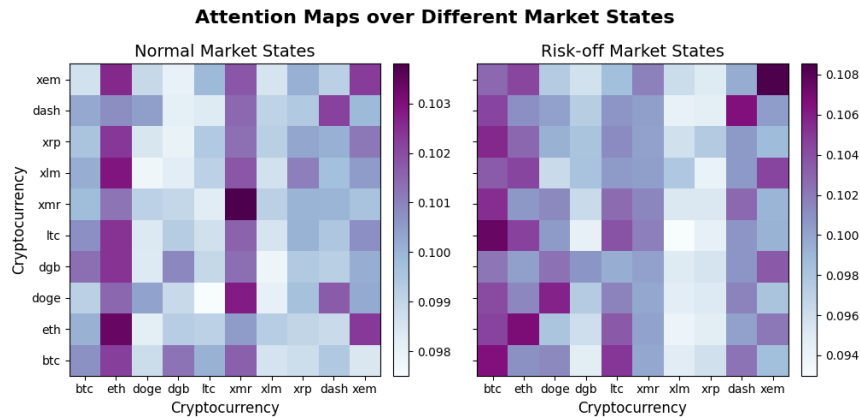


Figure 4: Aggregated attention heatmaps for the FEN model over both normal (left) and risk-off (right) periods. Localised groups of darker cells form across the map over normal states as measured by the VIX – likely reflecting idiosyncratic developments within the set of cryptocurrencies. The behaviour of the attention map under risk-off regimes, during which multiple cryptocurrencies are affected, is clearly reflected in the dispersion of darker shaded cells.

Table 4: Average weekly portfolio turnover across all strategies. FEN has the lowest turnover.

	Benchmarks						Proposed
	1WR	MLP	LN	LM	SAR	SAR+ps	FEN
Turnover	0.832	0.710±0.030	0.711±0.047	0.787±0.018	0.676±0.038	0.715±0.053	*0.673±0.039

Optimization. *Computational Science & Discovery* 8, 1 (July 2015), 014008. <https://doi.org/10.1088/1749-4699/8/1/014008>

[6] Stefano B. Blumberg, Marco Palombo, Can Son Khoo, Chantal M. W. Tax, Ryutaro Tanno, and Daniel C. Alexander. 2019. Multi-stage Prediction Networks for Data Harmonization. In *Medical Image Computing and Computer Assisted Intervention – MICCAI 2019*, Dinggang Shen, Tianming Liu, Terry M. Peters, Lawrence H. Staib, Caroline Essert, Sean Zhou, Pew-Thian Yap, and Ali Khan (Eds.). Vol. 11767.

Springer International Publishing, Cham, 411–419. https://doi.org/10.1007/978-3-030-32251-9_45 Series Title: Lecture Notes in Computer Science.

[7] Lorenzo Brigato and Luca Iocchi. 2020. A Close Look at Deep Learning with Small Data. In *25th International Conference on Pattern Recognition, ICPR 2020, Virtual Event / Milan, Italy, January 10-15, 2021*. IEEE, 2490–2497. <https://doi.org/10.1109/ICPR48806.2021.9412492>

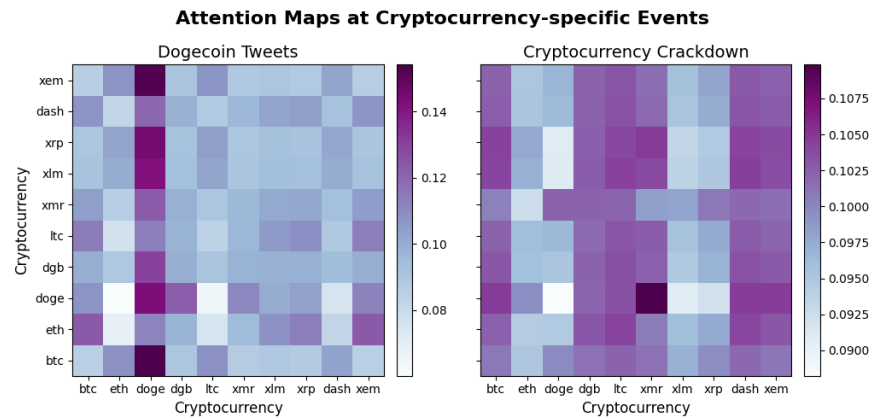


Figure 5: Aggregated attention heatmaps for the FEN model around the time of major cryptocurrency-related events. An activated column can be seen for Dogecoin around the time of Elon Musk’s tweets about the digital token during early May 2021 (left). The pattern of diffused shaded blocks in the second half of May 2021 coincides with China’s government regulators declaring a crack down on financial institutions’ use of cryptocurrencies and reflects the risk-off sentiments inherent in this event (right).

Table 5: Sharpe ratios across selected profitable strategies with a 15% annual volatility target under different transaction cost assumptions. Positive Sharpe ratios for FEN persists up to around 29 bps. This is above the 26 bps per trade assumed for cryptocurrencies and thus demonstrate their suitability for trading these instruments.

Transaction Costs	Benchmarks				Proposed
	1WR	MLP	LM	SAR	FEN
0 bps	0.238	0.403±0.240	0.456±0.546	0.496±0.583	*0.749±0.410
5 bps	0.115	0.273±0.248	0.302±0.542	0.360±0.580	*0.621±0.415
10 bps	-0.011	0.144±0.257	0.153±0.532	0.225±0.576	*0.493±0.418
15 bps	-0.140	0.016±0.267	0.11±0.515	0.089±0.574	*0.366±0.422
20 bps	-0.271	-0.111±0.276	-0.134±0.506	-0.046±0.571	*0.238±0.425
25 bps	-0.404	-0.236±0.286	-0.283±0.504	-0.180±0.569	*0.111±0.429
30 bps	-0.538	-0.359±0.297	-0.433±0.504	-0.315±0.567	*-0.017±0.432

[8] Sebastian Bruch, Masrour Zoghi, Michael Bendersky, and Marc Najork. 2019. Revisiting Approximate Metric Optimization in the Age of Deep Neural Networks. In *Proceedings of the 42nd International ACM SIGIR Conference on Research and Development in Information Retrieval*. ACM, Paris France, 1241–1244. <https://doi.org/10.1145/3331184.3331347>

[9] Christopher J. C. Burges. 2010. *From RankNet to LambdaRank to LambdaMART: An overview*. Technical Report MSR-TR-2010-82. Microsoft Research. http://research.microsoft.com/en-us/um/people/cburges/tech_reports/MSR-TR-2010-82.pdf

[10] Chris J. C. Burges, Krysta M. Svore, Qiang Wu, and Jianfeng Gao. 2008. *Ranking, boosting, and model adaptation*. Technical Report MSR-TR-2008-109. 18 pages. <https://www.microsoft.com/en-us/research/publication/ranking-boosting-and-model-adaptation/>

[11] Zhe Cao, Tao Qin, Tie-Yan Liu, Ming-Feng Tsai, and Hang Li. 2007. Learning to rank: from pairwise approach to listwise approach. In *Proceedings of the 24th international conference on Machine learning - ICML '07*. ACM Press, Corvallis, Oregon, 129–136. <https://doi.org/10.1145/1273496.1273513>

[12] Cboe Global Markets Cboe. 2022. VIX Historical Price Data. *Calculated (or Derived) based on Cboe data*. (2022). https://www.cboe.com/tradable_products/vix/vix_historical_data/

[13] Olivier Chapelle, Yi Chang, and Tie-Yan Liu. 2011. Future directions in learning to rank. In *Proceedings of the learning to rank challenge (Proceedings of machine learning research, Vol. 14)*, Olivier Chapelle, Yi Chang, and Tie-Yan Liu (Eds.). PMLR, Haifa, Israel, 91–100. <https://proceedings.mlr.press/v14/chapelle11b.html> <http://proceedings.mlr.press/v14/chapelle11b/chapelle11b.pdf>

[14] Olivier Chapelle, Pannagadatta Shivaswamy, Srinivas Vadrevu, Kilian Weinberger, Ya Zhang, and Belle Tseng. 2010. Multi-task learning for boosting with application to web search ranking. In *Proceedings of the 16th ACM SIGKDD international conference on Knowledge discovery and data mining - KDD '10*. ACM Press, Washington, DC, USA, 1189. <https://doi.org/10.1145/1835804.1835953>

[15] Depin Chen, Yan Xiong, Jun Yan, Gui-Rong Xue, Gang Wang, and Zheng Chen. 2010. Knowledge transfer for cross domain learning to rank. *Information Retrieval* 13, 3 (June 2010), 236–253. <https://doi.org/10.1007/s10791-009-9111-2>

[16] Keke Chen, Rongqing Lu, C. K. Wong, Gordon Sun, Larry Heck, and Belle Tseng. 2008. Trada: tree based ranking function adaptation. In *Proceeding of the 17th ACM conference on Information and knowledge mining - CIKM '08*. ACM Press, Napa Valley, California, USA, 1143. <https://doi.org/10.1145/1458082.1458233>

[17] Tianqi Chen and Carlos Guestrin. 2016. XGBoost: A Scalable Tree Boosting System. In *Proceedings of the 22nd ACM SIGKDD International Conference on Knowledge Discovery and Data Mining* (San Francisco, California, USA) (*KDD '16*). ACM, New York, NY, USA, 785–794. <https://doi.org/10.1145/2939672.2939785>

[18] Djork-Armé Clevert, Thomas Unterthiner, and Sepp Hochreiter. 2016. Fast and Accurate Deep Network Learning by Exponential Linear Units (ELUs). In *4th International Conference on Learning Representations, ICLR 2016, San Juan, Puerto Rico, May 2-4, 2016, Conference Track Proceedings*, Yoshua Bengio and Yann LeCun (Eds.). <http://arxiv.org/abs/1511.07289>

[19] CoinMarketCap. 2022. Cryptocurrency Prices, Charts And Market Capitalizations | CoinMarketCap. *Calculated (or Derived) based on CoinMarketCap data*. (2022). <https://coinmarketcap.com/>

[20] Wenyuan Dai, Gui-Rong Xue, Qiang Yang, and Yong Yu. 2007. Co-clustering based classification for out-of-domain documents. In *Proceedings of the 13th ACM SIGKDD international conference on Knowledge discovery and data mining - KDD '07*. ACM Press, San Jose, California, USA, 210. <https://doi.org/10.1145/1281192>

- 1281218
- [21] Oscar Day and Taghi M. Khoshgoftaar. 2017. A survey on heterogeneous transfer learning. *Journal of Big Data* 4, 1 (Dec. 2017), 29. <https://doi.org/10.1186/s40537-017-0089-0>
- [22] Jacob Devlin, Ming-Wei Chang, Kenton Lee, and Kristina Toutanova. 2019. BERT: Pre-training of deep bidirectional transformers for language understanding. In *Proceedings of the 2019 conference of the north american chapter of the association for computational linguistics: Human language technologies, NAACL-HLT 2019, minneapolis, MN, USA, june 2-7, 2019, volume 1 (long and short papers)*, Jill Burstein, Christy Doran, and Thamar Solorio (Eds.). Association for Computational Linguistics, 4171–4186. <https://doi.org/10.18653/v1/n19-1423> tex.bibsource: dblp computer science bibliography, <https://dblp.org> tex.biburl: <https://dblp.org/rec/conf/naacl/DevlinCLT19.bib> tex.timestamp: Fri, 06 Aug 2021 00:41:31 +0200.
- [23] Chuong B. Do and Andrew Y. Ng. 2005. Transfer learning for text classification. In *Advances in neural information processing systems*, Y. Weiss, B. Schölkopf, and J. Platt (Eds.), Vol. 18. MIT Press. <https://proceedings.neurips.cc/paper/2005/file/bf2fb7d1825a1df3ca308ad0bf48591e-Paper.pdf>
- [24] Steven Feng, Varun Gangal, Jason Wei, Sarath Chandar, Soroush Vosoughi, Teruko Mitamura, and Eduard Hovy. 2021. A Survey of Data Augmentation Approaches for NLP. In *Findings of the Association for Computational Linguistics: ACL-IJCNLP 2021*. Association for Computational Linguistics, Online, 968–988. <https://doi.org/10.18653/v1/2021.findings-acl.84>
- [25] Jianfeng Gao, Qiang Wu, Chris Burges, Krysta Svore, Yi Su, Nazan Khan, Shalin Shah, and Hongyan Zhou. 2009. Model adaptation via model interpolation and boosting for web search ranking. In *Proceedings of the 2009 Conference on Empirical Methods in Natural Language Processing Volume 2 - EMNLP '09*, Vol. 2. Association for Computational Linguistics, Singapore, 505. <https://doi.org/10.3115/1699571.1699578>
- [26] Wei Gao, Peng Cai, Kam-Fai Wong, and Aoying Zhou. 2010. Learning to rank only using training data from related domain. In *Proceeding of the 33rd international ACM SIGIR conference on Research and development in information retrieval - SIGIR '10*. ACM Press, Geneva, Switzerland, 162. <https://doi.org/10.1145/1835449.1835478>
- [27] Ross Girshick, Jeff Donahue, Trevor Darrell, and Jitendra Malik. 2014. Rich feature hierarchies for accurate object detection and semantic segmentation. In *Proceedings of the 2014 IEEE conference on computer vision and pattern recognition (CVPR '14)*. IEEE Computer Society, USA, 580–587. <https://doi.org/10.1109/CVPR.2014.81> Number of pages: 8.
- [28] Shihao Gu, Bryan T. Kelly, and Dacheng Xiu. 2019. Autoencoder Asset Pricing Models. *SSRN Electronic Journal* (2019). <https://doi.org/10.2139/ssrn.3335536>
- [29] Thomas Hale, Tabby Kinder, and Philip Stafford. 2021. Bitcoin gyrates on fears of regulatory crackdown. *Financial Times* (May 2021). <https://www.ft.com/content/c4c29bb3-c8ee-454c-a2dd-eac9f644007f>
- [30] Qi-Qiao He, Patrick Cheong-Iao Pang, and Yain-Whar Si. 2019. Transfer Learning for Financial Time Series Forecasting. In *PRICAI 2019: Trends in Artificial Intelligence*, Abhaya C. Nayak and Alok Sharma (Eds.), Vol. 11671. Springer International Publishing, Cham, 24–36. https://doi.org/10.1007/978-3-030-29911-8_3 Series Title: Lecture Notes in Computer Science.
- [31] Jeremy Howard and Sebastian Ruder. 2018. Universal Language Model Fine-tuning for Text Classification. In *Proceedings of the 56th Annual Meeting of the Association for Computational Linguistics (Volume 1: Long Papers)*. Association for Computational Linguistics, Melbourne, Australia, 328–339. <https://doi.org/10.18653/v1/P18-1031>
- [32] Kalervo Järvelin and Jaana Kekäläinen. 2000. IR Evaluation Methods for Retrieving Highly Relevant Documents. In *Proceedings of the 23rd Annual International ACM SIGIR Conference on Research and Development in Information Retrieval - SIGIR '00*. ACM Press, Athens, Greece, 41–48. <https://doi.org/10.1145/345508.345545>
- [33] Narasimhan Jegadeesh and Sheridan Titman. 1993. Returns to Buying Winners and Selling Losers: Implications for Stock Market Efficiency. *The Journal of Finance* 48, 1 (March 1993), 65–91. <https://doi.org/10.1111/j.1540-6261.1993.tb04702.x>
- [34] Gyeen Jeong and Ha Young Kim. 2019. Improving financial trading decisions using deep Q-learning: Predicting the number of shares, action strategies, and transfer learning. *Expert Systems with Applications* 117 (March 2019), 125–138. <https://doi.org/10.1016/j.eswa.2018.09.036>
- [35] Saejoon Kim. 2019. Enhancing the momentum strategy through deep regression. *Quantitative Finance* 19, 7 (July 2019), 1121–1133. <https://doi.org/10.1080/14697688.2018.1563707> tex.ids: kimEnhancingMomentumStrategy2019.
- [36] Alexander Kolesnikov, Lucas Beyer, Xiaohua Zhai, Joan Puigcerver, Jessica Yung, Sylvain Gelly, and Neil Houlsby. 2020. Big Transfer (BiT): General Visual Representation Learning. In *Computer Vision – ECCV 2020*, Andrea Vedaldi, Horst Bischof, Thomas Brox, and Jan-Michael Frahm (Eds.), Vol. 12350. Springer International Publishing, Cham, 491–507. https://doi.org/10.1007/978-3-030-58558-7_29 Series Title: Lecture Notes in Computer Science.
- [37] Simon Kornblith, Jonathon Shlens, and Quoc V. Le. 2019. Do Better ImageNet Models Transfer Better?. In *2019 IEEE/CVF Conference on Computer Vision and Pattern Recognition (CVPR)*. IEEE, Long Beach, CA, USA, 2656–2666. <https://doi.org/10.1109/CVPR.2019.00277>
- [38] Adriano Koshiyama, Stefano B. Blumberg, Nick Firoozye, Philip Treleven, and Sebastian Flennerhag. 2021. QuantNet: transferring learning across trading strategies. *Quantitative Finance* (Dec. 2021), 1–20. <https://doi.org/10.1080/14697688.2021.1999487>
- [39] Hang Li. 2011. Learning to Rank for Information Retrieval and Natural Language Processing. *Synthesis Lectures on Human Language Technologies* 4, 1 (April 2011), 1–113. <https://doi.org/10.2200/S00348ED1V01Y201104HLT012>
- [40] Pengfei Li. 2019. *Transfer learning for information retrieval*. Ph.D. Dissertation. RMIT University.
- [41] Pengfei Li, Mark Sanderson, Mark Carman, and Falk Scholer. 2020. Self-labeling methods for unsupervised transfer ranking. *Information Sciences* 516 (April 2020), 293–315. <https://doi.org/10.1016/j.ins.2019.12.067>
- [42] Tie-Yan Liu. 2011. *Transfer Ranking*. In *Learning to Rank for Information Retrieval*. Springer Berlin Heidelberg, Berlin, Heidelberg, 127–130. https://doi.org/10.1007/978-3-642-14267-3_9
- [43] Mingsheng Long, Yue Cao, Jianmin Wang, and Michael I. Jordan. 2015. Learning transferable features with deep adaptation networks. In *Proceedings of the 32nd international conference on international conference on machine learning - volume 37 (ICML '15)*. JMLR.org, 97–105. Place: Lille, France Number of pages: 9.
- [44] Lukas Menkhoff, Lucio Sarno, Maik Schmeling, and Andreas Schrimpf. 2012. Currency momentum strategies. *Journal of Financial Economics* 106, 3 (Dec. 2012), 660–684. <https://doi.org/10.1016/j.jfineco.2012.06.009>
- [45] Kei Nakagawa, Masaya Abe, and Junpei Komiya. 2020. A Robust Transferable Deep Learning Framework for Cross-sectional Investment Strategy. *2020 IEEE 7th International Conference on Data Science and Advanced Analytics (DSAA)* (Oct. 2020), 370–379. <https://doi.org/10.1109/DSAA49011.2020.00051> arXiv: 1910.01491.
- [46] Sinno Jialin Pan and Qiang Yang. 2010. A Survey on Transfer Learning. *IEEE Transactions on Knowledge and Data Engineering* 22, 10 (Oct. 2010), 1345–1359. <https://doi.org/10.1109/TKDE.2009.191> Conference Name: IEEE Transactions on Knowledge and Data Engineering.
- [47] Zizheng Pan, Bohan Zhuang, Haoyu He, Jing Liu, and Jianfei Cai. 2021. Less is More: Pay Less Attention in Vision Transformers. <http://arxiv.org/abs/2105.14217> Number: arXiv:2105.14217 arXiv:2105.14217 [cs].
- [48] Changhua Pei, Yi Zhang, Yongfeng Zhang, Fei Sun, Xiao Lin, Hanxiao Sun, Jian Wu, Peng Jiang, and Wenwu Ou. 2019. Personalized Re-ranking for Recommendation. *arXiv:1904.06813 [cs]* (July 2019). <http://arxiv.org/abs/1904.06813> arXiv: 1904.06813.
- [49] Przemyslaw Pobrotyn, Tomasz Bartczak, Mikołaj Synowiec, Radosław Białobrzęski, and Jarosław Bojar. 2020. Context-Aware Learning to Rank with Self-Attention. In *arXiv:2005.10084 [cs] (SIGIR eCom '20)*. Virtual Event China. <http://arxiv.org/abs/2005.10084> arXiv: 2005.10084.
- [50] Daniel Poh, Bryan Lim, Stefan Zohren, and Stephen Roberts. 2021. Building Cross-Sectional Systematic Strategies by Learning to Rank. *The Journal of Financial Data Science* (March 2021), 70–86. <https://doi.org/10.3905/jfds.2021.1.060>
- [51] Daniel Poh, Bryan Lim, Stefan Zohren, and Stephen Roberts. 2022. Enhancing Cross-Sectional Currency Strategies by Context-Aware Learning to Rank with Self-Attention. *arXiv:2105.10019 [cs, q-fin]* (Jan. 2022). <http://arxiv.org/abs/2105.10019> arXiv: 2105.10019.
- [52] Zhen Qin, Le Yan, Honglei Zhuang, Yi Tay, Rama Kumar Pasumarthi, Xuanhui Wang, Mike Bendersky, and Marc Najork. 2021. Are neural rankers still outperformed by gradient boosted decision trees?. In *International conference on learning representations (ICLR)*.
- [53] Ali Sharif Razavian, Hossein Azizpour, Josephine Sullivan, and Stefan Carlsson. 2014. CNN Features Off-the-Shelf: An Astounding Baseline for Recognition. In *2014 IEEE Conference on Computer Vision and Pattern Recognition Workshops*. 512–519. <https://doi.org/10.1109/CVPRW.2014.131> ISSN: 2160-7516.
- [54] Sofia Serrano and Noah A. Smith. 2019. Is Attention Interpretable?. In *Proceedings of the 57th Annual Meeting of the Association for Computational Linguistics*. Association for Computational Linguistics, Florence, Italy, 2931–2951. <https://doi.org/10.18653/v1/P19-1282>
- [55] Zhiqiang Shen, Zechun Liu, Jie Qin, Marios Savvides, and Kwang-Ting Cheng. 2021. Partial is better than all: Revisiting fine-tuning strategy for few-shot learning. In *Thirty-fifth AAAI conference on artificial intelligence, AAAI 2021, thirty-third conference on innovative applications of artificial intelligence, IAAI 2021, the eleventh symposium on educational advances in artificial intelligence, EAAI 2021, virtual event, february 2-9, 2021*. AAAI Press, 9594–9602. <https://ojs.aaai.org/index.php/AAAI/article/view/17155> tex.bibsource: dblp computer science bibliography, <https://dblp.org> tex.biburl: <https://dblp.org/rec/conf/aaai/SheenLQSC21.bib> tex.timestamp: Sat, 05 Jun 2021 18:11:55 +0200.
- [56] Connor Shorten and Taghi M. Khoshgoftaar. 2019. A survey on Image Data Augmentation for Deep Learning. *Journal of Big Data* 6, 1 (Dec. 2019), 60. <https://doi.org/10.1186/s40537-019-0197-0>
- [57] Hendra Suryanto, Charles Guan, Andrew Voumard, and Ghassan Beydoun. 2019. Transfer learning in credit risk. In *Machine learning and knowledge discovery in databases - european conference, ECML PKDD 2019, wüzburg, germany, september*

- 16-20, 2019, *proceedings, part III (Lecture notes in computer science, Vol. 11908)*, Ulf Brefeld, Élisia Fromont, Andreas Hotho, Arno J. Knobbe, Marloes H. Maathuis, and Céline Robardet (Eds.). Springer, 483–498. https://doi.org/10.1007/978-3-030-46133-1_29 tex.bibsource: dblp computer science bibliography, <https://dblp.org> tex.biburl: <https://dblp.org/rec/conf/pkdd/SuryantoGVB19.bib> tex.timestamp: Fri, 22 May 2020 21:56:37 +0200.
- [58] Panagiotis Tzouvanas, Renatas Kizys, and Bayasgalan Tsend-Ayush. 2020. Momentum trading in cryptocurrencies: Short-term returns and diversification benefits. *Economics Letters* 191 (June 2020), 108728. <https://doi.org/10.1016/j.econlet.2019.108728>
- [59] Godfrey Uzonwanne. 2021. Volatility and return spillovers between stock markets and cryptocurrencies. *The Quarterly Review of Economics and Finance* 82 (Nov. 2021), 30–36. <https://doi.org/10.1016/j.qref.2021.06.018>
- [60] Ashish Vaswani, Noam Shazeer, Niki Parmar, Jakob Uszkoreit, Llion Jones, Aidan N. Gomez, unreviewed Kaiser, and Illia Polosukhin. 2017. Attention is all you need. In *Proceedings of the 31st international conference on neural information processing systems (NIPS'17)*. Curran Associates Inc., Red Hook, NY, USA, 6000–6010. Number of pages: 11 Place: Long Beach, California, USA.
- [61] Hongning Wang, Xiaodong He, Ming-Wei Chang, Yang Song, Ryen W. White, and Wei Chu. 2013. Personalized ranking model adaptation for web search. In *Proceedings of the 36th international ACM SIGIR conference on Research and development in information retrieval*. ACM, Dublin Ireland, 323–332. <https://doi.org/10.1145/2484028.2484068>
- [62] Jindong Wang, Cuiling Lan, Chang Liu, Yidong Ouyang, Tao Qin, Wang Lu, Yiqiang Chen, Wenjun Zeng, and Philip S. Yu. 2021. Generalizing to Unseen Domains: A Survey on Domain Generalization. *arXiv:2103.03097 [cs]* (Dec. 2021). <http://arxiv.org/abs/2103.03097> arXiv: 2103.03097.
- [63] Liang Wang and Khaled Rasheed. 2018. Stock ranking with market microstructure, technical indicator and news. In *Proceedings on the international conference on artificial intelligence (ICAI)*. 322–328. <https://csce.ucmss.com/cr/books/2018/LFS/CSREA2018/ICA3687.pdf> tex.organization: The Steering Committee of The World Congress in Computer Science, Computer ...
- [64] Ruoxi Wang, Rakesh Shivanna, Derek Cheng, Sagar Jain, Dong Lin, Lichan Hong, and Ed Chi. 2021. DCN V2: Improved deep & cross network and practical lessons for web-scale learning to rank systems. In *Proceedings of the web conference 2021 (WWW '21)*. Association for Computing Machinery, New York, NY, USA, 1785–1797. <https://doi.org/10.1145/3442381.3450078> Number of pages: 13 Place: Ljubljana, Slovenia.
- [65] Yaqing Wang, Quanming Yao, James T. Kwok, and Lionel M. Ni. 2021. Generalizing from a Few Examples: A Survey on Few-shot Learning. *Comput. Surveys* 53, 3 (May 2021), 1–34. <https://doi.org/10.1145/3386252>
- [66] Karl Weiss, Taghi M. Khoshgoftaar, and DingDing Wang. 2016. A survey of transfer learning. *Journal of Big Data* 3, 1 (Dec. 2016), 9. <https://doi.org/10.1186/s40537-016-0043-6>
- [67] Tom Westbrook and Tom Wilson. 2021. Musk tweets, dogecoin leaps and bitcoin retreats. *Reuters* (May 2021). <https://www.reuters.com/technology/dogecoin-pops-after-musk-tweets-about-promising-system-improvements-2021-05-13/>
- [68] Fen Xia, Tie-Yan Liu, Jue Wang, Wensheng Zhang, and Hang Li. 2008. Listwise approach to learning to rank: Theory and algorithm. In *Proceedings of the 25th international conference on machine learning (ICML '08)*. Association for Computing Machinery, New York, NY, USA, 1192–1199. <https://doi.org/10.1145/1390156.1390306> Number of pages: 8 Place: Helsinki, Finland.
- [69] Zihao Zhang, Stefan Zohren, and Stephen Roberts. 2019. DeepLOB: Deep Convolutional Neural Networks for Limit Order Books. *IEEE Transactions on Signal Processing* 67, 11 (June 2019), 3001–3012. <https://doi.org/10.1109/TSP.2019.2907260> arXiv:1808.03668 [q-fin].
- [70] Fuzhen Zhuang, Zhiyuan Qi, Keyu Duan, Dongbo Xi, Yongchun Zhu, Hengshu Zhu, Hui Xiong, and Qing He. 2019. A comprehensive survey on transfer learning. *CoRR* abs/1911.02685 (2019). <http://arxiv.org/abs/1911.02685> arXiv: 1911.02685 tex.bibsource: dblp computer science bibliography, <https://dblp.org> tex.biburl: <https://dblp.org/rec/journals/corr/abs-1911-02685.bib> tex.timestamp: Sat, 29 Aug 2020 18:19:14 +0200.

A LEARNING TO RANK AND TRANSFER RANKING

A.1 Learning to Rank for Cross-Sectional Momentum

Learning to Rank (LTR) is a supervised learning problem where the goal is to sort a list of objects to maximise some measure of utility (for e.g., discounted cumulative gain). For training, we are presented with a set of dates $\mathcal{B} = \{b_1, \dots, b_{t-1}\}$ where at each b_i

we have n instruments $\mathbf{c}_i = \{c_i^{(1)}, \dots, c_i^{(n)}\}$. We also have a corresponding set of quintiles Q of realised returns \mathbf{q}_{i+1} from the *next* period that \mathbf{c}_i have been assigned based on an ascending sort. Here, $\mathbf{q}_{i+1} = \{q_{i+1}^{(1)}, \dots, q_{i+1}^{(n)}\}$ where $q_{i+1}^{(j)} \in Q = \{Q_1, \dots, Q_5\}$ for $\forall i, j$. Additionally, $k > l \Rightarrow Q_k > Q_l$ for $k, l \in \{1, \dots, 5\}$ where $>$ stands for the order relation. In other words, instruments possessing higher realised returns are assigned higher quintiles. With each rebalance-instrument pair at period i , a feature vector $\mathbf{u}_i^{(j)} = \phi(b_i, c_i^{(j)})$ can be formed, noting that $\phi(\cdot)$ characterises the feature function and that $i \in \{1, \dots, t\}$ and $j \in \{1, \dots, n\}$. Letting $\mathbf{u}_i = \{u_i^{(1)}, \dots, u_i^{(n)}\}$, we can go on to form the broader training set $\{\mathbf{u}_i, \mathbf{q}_{i+1}\}_{i=1}^{t-1}$. The goal of LTR is to learn a function f that predicts a score $f(\mathbf{u}_i^{(j)}) = z_i^{(j)}$ at the Score Calculation phase (refer to the Traditional LTR pipeline in Figure 1) when presented with an out-of-sample input $\mathbf{u}_i^{(j)}$. For more details, we point the reader to [50] and [39].

A.2 From Learning to Rank to Transfer Ranking

Transfer Ranking (TR) builds on top of the LTR framework. A *domain* \mathcal{D} consists of a feature space \mathcal{X} and a marginal distribution $P(X)$, i.e., $\mathcal{D} = \{\mathcal{X}, P(X)\}$. X represents an instance set and is defined as $X = \{\mathbf{x}|x_i \in \mathcal{X}, i = 1, \dots, n\}$. A *task* \mathcal{T} is composed of a label space \mathcal{Y} and a decision function f , so $\mathcal{T} = \{\mathcal{Y}, f\}$. The decision function f is learned from the data. Using these definitions, the goal of LTR for CSM in Section A.1 can be expressed as learning the ranking function f in $\mathcal{T} = \{Q, f\}$ over some domain of interest $\mathcal{D} = \{\mathcal{U}, P(U)\}$. The feature space and instance set are represented by \mathcal{U} and U respectively. A single instance \mathbf{u}_i at period i is given as $\mathbf{u}_i = \{u_i^{(1)}, \dots, u_i^{(n)}\}$ where $u_i^{(j)} \in \mathcal{U}$ for $\forall i, j$.

In the TR setting, we are given observations corresponding to $m^S \in \mathbb{N}^+$ *source* domains and tasks, i.e., $\{(\mathcal{D}_{S_i}, \mathcal{T}_{S_i}) \mid i = 1, \dots, m^S\}$ as well as observations about $m^T \in \mathbb{N}^+$ *target* domains and tasks, i.e., $\{(\mathcal{D}_{T_j}, \mathcal{T}_{T_j}) \mid j = 1, \dots, m^T\}$. TR aims to exploit the knowledge embedded in the source domains to enhance the performance of the learned decision functions $f_{T_j}, j = 1, \dots, m^T$ on the target domains. In this work, we focus on $m^S = m^T = 1$. Specifically, we want to enhance the performance of f_T , which is the scoring function for cryptocurrencies, by incorporating knowledge extracted from the FX dataset f_S . This is achieved by sharing the parameters θ_S of the calibrated f_S with f_T as described in Section 3.

B DATASET DETAILS

B.1 Source Dataset

Our source dataset is composed of 31 currencies all expressed versus the USD over the period 2-May-2000 to 31-Dec-2021. We make use of this data to train the upstream model required for knowledge transfer. The full list of currencies is as follows:

- G10: AUD, CAD, CHF, EUR, GBP, JPY, NOK, NZD, SEK, USD
- EM Asia: HKD, INR, IDR, KRW, MYR, PHP, SGD, TWD, THB
- EM Latam: BRL, CLP, COP, PEN, MXN
- CEEMEA: CZK, HUF, ILS, PLN, RUB, TRY
- Africa: ZAR

B.2 Target Dataset

Our target dataset is focused on the following 10 cryptocurrencies: Bitcoin (BTC), Ethereum (ETH), DogeCoin (DOGE), DigiByte (DGB), Litecoin (LTC), Stellar (XLM), XRP, Monero (XMR), NEM (XEM), Dash (DASH). The dataset for these digital tokens span 1-Jan-2016 to 31-Dec-2021.

B.3 Data Preprocessing

In order to reduce the impact of outliers during training, we winsorise both foreign exchange and cryptocurrency data by capping and flooring it to be within 3 times its exponentially weighted moving (EWM) standard deviation from its EWM average that is calculated with a 26-week halflife decay.

C ADDITIONAL TRAINING DETAILS

Model Fine-tuning: We fine-tune both FEN and SAR+ps models. In this step, we unfreeze the entire network and re-train with the lowest value in the learning rate search range, i.e., 10^{-6} and over different batch sizes.

Python Libraries: LambdaMART uses XGBoost [17]. All other machine learning models are developed with TensorFlow [1].

Hyperparameter Optimisation: Hyperparameters are tuned using HyperOpt [5]. For LambdaMART, we refer to the hyperparameters as they are named in the XGBoost library. The feature search spaces for various machine learning models are as follows:

Multi-layer Perceptron (MLP):

- Dropout Rate – [0.0, 0.2, 0.4, 0.6, 0.8]
- Hidden Width – [8, 16, 32, 64, 128]
- Batch Size – [8, 16, 32, 64, 128]
- Learning Rate – [10^{-6} , 10^{-5} , 10^{-4} , 10^{-3} , 10^{-2} , 10^{-1}]

ListNet (LN):

- Dropout Rate – [0.0, 0.2, 0.4, 0.6, 0.8]
- Hidden Width – [8, 16, 32, 64, 128]
- Batch Size – [1, 2, 4, 8, 16]
- Learning Rate – [10^{-6} , 10^{-5} , 10^{-4} , 10^{-3}]

LambdaMART (LM):

- ‘objective’ – ‘rank:pairwise’
- ‘eval_metric’ – ‘ndcg’
- ‘num_boost_round’ – [50, 100, 250, 500, 1000]
- ‘max_depth’ – [6, 7, 8, 9, 10]
- ‘eta’ – [10^{-6} , 10^{-5} , 10^{-4} , 10^{-3} , 10^{-2} , 10^{-1}]
- ‘reg_alpha’ – [10^{-6} , 10^{-5} , 10^{-4} , 10^{-3} , 10^{-2} , 10^{-1}]
- ‘reg_lambda’ – [10^{-6} , 10^{-5} , 10^{-4} , 10^{-3} , 10^{-2} , 10^{-1}]
- ‘tree_method’ – ‘gpu_hist’

Self-attention Ranker (SAR), Self-attention Ranker with Parameter-sharing (SAR+ps), both the source model for Fused Encoder Networks (FEN) and FEN itself:

- d_{fc} – [8, 16, 32, 64, 128]
- d_{ff} – [8, 16, 32, 64, 128]
- Dropout Rate – [0.0, 0.2, 0.4, 0.6, 0.8]
- Hidden Width – [16, 32, 64, 128, 256]
- Batch Size – [2, 4, 6, 8, 10]

Table 6: Performance metrics for FEN and SAR+ps over the 2018-2021 period with a 15% annual volatility target. All figures are based on 10 runs. Both models incorporate components from *sub-optimal* source models. The impact is clearly evident for both models with statistics that are worse off than their respective counterparts in Table 1.

	SAR+ps	FEN
E[returns]	-0.050±0.097	0.078±0.055
Volatility	0.174±0.013	0.190±0.018
Sharpe Ratio	-0.277±0.569	0.414±0.302
Sortino Ratio	-0.260±0.819	0.719±0.527
Calmar Ratio	-0.009±0.321	0.364±0.264
Downside Deviation	0.131±0.025	0.117±0.018
Max. Drawdown	-0.424±0.173	0.240±0.066
Avg. Profit / Avg. Loss	1.016±0.249	1.189±0.163
Hit Rate	0.459±0.026	0.496±0.020

- Learning Rate – [10^{-6} , 10^{-5} , 10^{-4} , 10^{-3}]
- No. of Encoder Layers – [1, 2, 3, 4]
- No. of Attention Heads – 1

Fine-tuning step for SAR+ps and FEN:

- Batch Size – [2, 4, 6, 8, 10]
- Learning Rate – 10^{-6}

D INCORPORATING KNOWLEDGE FROM SUB-OPTIMAL SOURCE MODELS

We investigate the impact on model performance when inappropriate source models are used for knowledge transfer. Out of 10 runs of the source model, we pick the *worst* 2 as measured by the strategy’s Sharpe ratio on the out-of-sample period. Using components from each, we construct their respective target models and make predictions on the corresponding target dataset. The results of this exercise are presented in Table 6. Importantly, we see that transferring knowledge from sub-optimal source models has a substantial performance drag for FEN (around 45% reduction in the Sharpe ratio).

E COMPARING ATTENTION HEATMAPS

This section compares the heatmaps of models that make use of the attention mechanism, namely, the SAR, SAR+ps and FEN. Specifically, for each market state and cryptocurrency-specific event discussed in Section 5.5.3, we present the weights of each model’s last attention layer. Darker cells correspond to larger weights which contribute more to the model’s prediction. Additionally, attention weights across different models are *not* comparable since these are raw weights. Overall, the patterns produced by FEN appears to broadly align with what one might expect. Risk-off states, for instance, are associated with heatmaps with darker cells that are dispersed – reflecting the broad impact felt by multiple instruments. This development is observed to a lesser extent in SAR, and is almost completely absent in SAR+ps.

Attention Maps across Models over Normal Market States

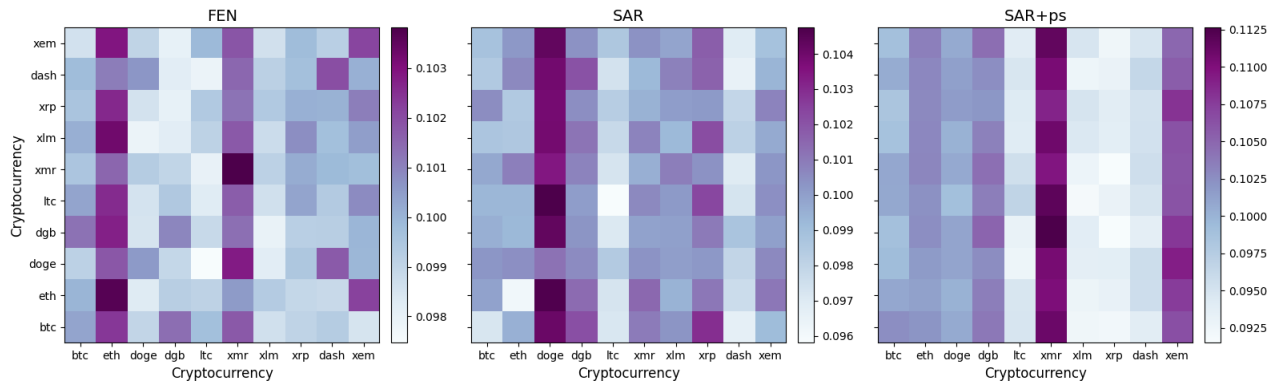


Figure 6: Aggregated maps over normal market states. Cells with larger weights cluster in pockets for FEN, but are dispersed for SAR. SAR+ps interestingly places high amount of attention weights on Monero ('xmr') and NEM ('xem'), which are relatively less popular than Bitcoin ('btc') and Ethereum ('eth').

Attention Maps across Models over Risk-off Market States

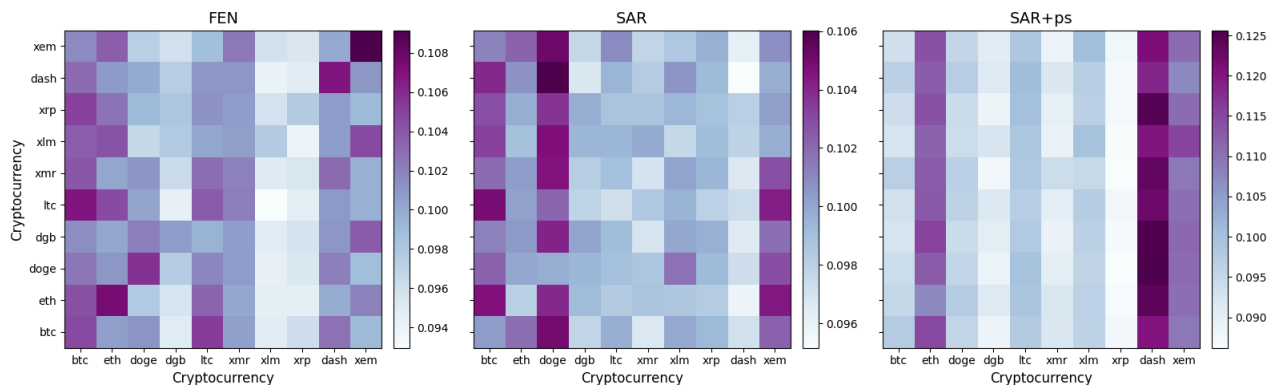


Figure 7: Aggregated maps over risk-off market states. Darker cells are more dispersed in FEN and SAR, but less so for SAR+ps.

Attention Maps across Models (Dogecoin Tweets)

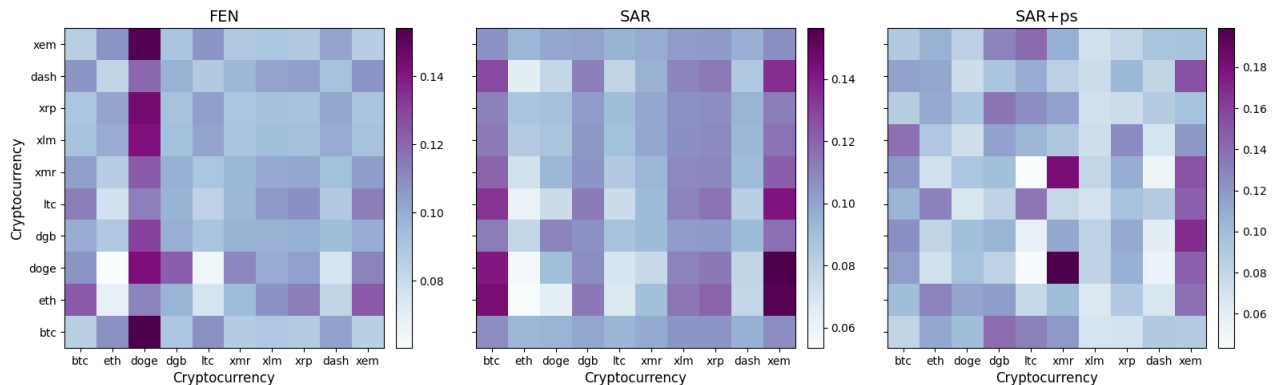


Figure 8: Attention maps in early May 2021, around the time of Elon Musk's Dogecoin ('doge') tweets. The 'doge' column is activated for FEN, but this pattern is absent for both SAR and SAR+ps.

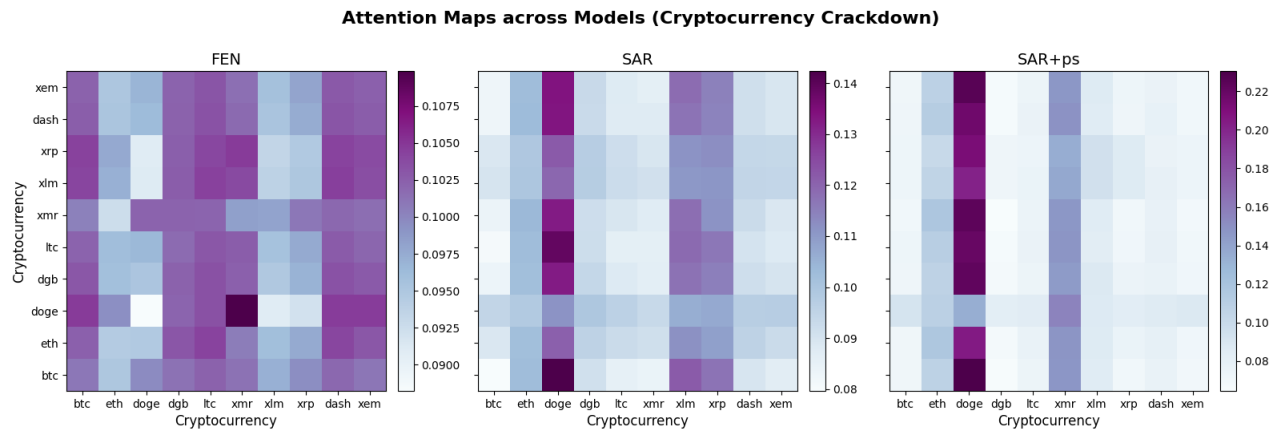


Figure 9: Attention maps for the second half of May 2021, which covers China’s government regulators declaring a crack down on the use of of cryptocurrencies by domestic financial institutions on the 19th of the same month. The significance of this event is evident from the pattern of diffused shaded blocks for FEN, with multiple coins affected. This is observed to a lesser extent in SAR’s attention map, and is almost completely absent in SAR+ps’s.